AEROSPACE SYMPOSIUM ONERA/DLR PARIS June 2001

Realistic Radar Simulation package Applied to Multisensor Scenarios

H.J. MAMETSA[1], T. CATHALA[2], A. BERGES[1], J. LATGER[2]

1: ONERA-CERT/DEMR
2, av. E. Belin, BP 4025 31055 Toulouse Cedex France
Phone: 33 5 62 25 27 07 email: mametsa@onecert.fr

2: Société OKTAL SE
2, rue Boudeville 31100 Toulouse France
Phone: 33 5 62 11 50 25 email: cathala@oktal.fr

ABSTRACT

A three dimensional (3-D) realistic radar simulation package applied to multisensor scenarios is under development as a project between the Electromagnetism and Radar Department of ONERA and the OKTAL SE Company. Taking advantage of various studies in the domain, this partnership associates the expertise of ONERA in radar phenomenology, millimetre wave interaction with targets and clutter, with that of OKTAL SE in the generation and management of realistic scene databases in the infrared and optical domains using advanced Shooting and Bouncing Rays (SBR) techniques [1, 2, 3]. The objective of this program is to develop simulation tools capable of predicting the behaviour of sensors in a realistic environment. This is achieved by coupling a terrain database completed by radar and optical features and a fast SBR algorithm. This paper is focused on the specification of the radar (i.e. electromagnetic wave interaction) principles. Various outputs from the simulations illustrate the effectiveness of the tool in respectively, Radar Cross Section (RCS) calculations, Synthetic Aperture Radar (SAR) simulations; and in the multisensor evaluation context in airborne applications (enhanced vision in airport application and target detection in conflictual context).

Purpose

Multiple applications could be created from the basic principles investigated in this project. This paper deals with the possibility of calculating multiple radar interactions in a realistic database. Applications include development and evaluation of new detection and signal processing algorithms to carry out ergonomic study. Simulation parameters take into account equipment potentialities, the sensitivity to meteorological effects and moving or non-moving target discrimination. For example, a specific purpose is to simulate the response of airborne multisensor equipment to determine the operational contribution of millimetre wave radar coupled with infrared and optical sensors according to a particular scenario. The display set up is comparable with the same one achieved by a specific airborne radar. This paper sets out a specification of the radar principles and examines the results of the first simulations in a realistic environment. Operational simulation of the millimetre wave sensor enables us to specify, evaluate, qualify and test the performances and limits of such future systems. To illustrate the effectiveness of the tool for performing research in this field, a variety of imagery output from the simulations is shown.

TECHNICAL FEATURES

Geometrical realistic database

For the principal airborne application presented in this paper, simulations are achieved using geometrical database which represents a numerical model of terrain, relatively undulating, rich in woodlands vegetation, and isolated trees. The database is composed of a very accurate high-resolution central area and a surrounding area at a lower resolution. The database is automatically generated using a terrain modelling tool (OKTAL SE product) from geographical data and paper maps.

This central area represents a 5 km x 7 km rectangular terrain, containing plane surfaces (crop fields, meadows, forests, lake), linear elements (roads, river) and punctual items (trees, man-made constructions, bridge, pylons with electrical wires). It is described by 200,000 polygons.

The central area is enclosed by a 20 km x 20 km surrounding domain, which is made up of fields, a lake and a river. This environment is described by 7,000 polygons.

Interesting facetted targets, fixed or in motion, land or airborne could be positioned in this scene.

Optical and infrared features

On figure 1, a part of a scene from the database is shown. Other databases have been developed for specific application such as enhanced vision in the airport of the future project.

Specific features and textures related to infrared, optics and radar are provided for each polygon of the scene database and for each polygon of the targets.

Figure 1: Part of a scene from the database

Radar features

For radar analysis, two classes of materials have been defined: the metallic materials and the environmental clutter with a predominance of specular and scattering effects. Each category of clutter is characterised by its backscattering coefficient average σ_0, which depends on the incidence angle and polarisation components (HH, VV, VH, and HV). Metallic materials (steel, aluminium) follow the Fresnel reflection coefficients $R_{\perp}$ and $R_{//}$ (respectively equal to –1 and + 1 for the electric field). The plane wave and clutter or target (composed essentially of metallic structure) interaction is specified below.

SHOOTING AND BOUNCING RAYS TECHNIQUE

In optical and infrared domains

Each polygon of the 3D scene is characterised by :

- physical attributes such as : spectral emissivity, spectral diffuse and specular BRDF; and spectral transmission (for non opaque materials),

- thermal attributes such as : conductivity, density, specific heat, thickness, convection coefficient, which allow computing the temperature of each polygon using thermal software.

An optronic (visible and infrared) model is implemented in our SBR algorithm. For each intersection between the 3D scene and each ray cast, it takes into account thermal emission, diffuse and specular reflection of the sun and diffuse reflection of the sky; and effects of atmospheric propagation.

In radar applications

The shooting ray technique is well adapted to this purpose. A set of rays representing the incident plane wave is shot toward the observed area composed by target and/or clutter (see figure 2). More specifically, from an emission point, this area is included in a cone in which elementary tubes of four rays are launched. Every tube is defined so that their intersection with the target (respectively the environmental clutter) constitutes a planar surface (respectively the same category of clutter). When a dense grid of uniform geometrical optics rays (10 rays per wavelength) is shot [4], an efficient algorithm of antialiasing [1], implemented in our SBR technique, drastically decreases the shooting ray number. A fast Radar Cross Section (RCS) analysis of complex 3-D perfectly conducting targets was carried out using this approach [5].

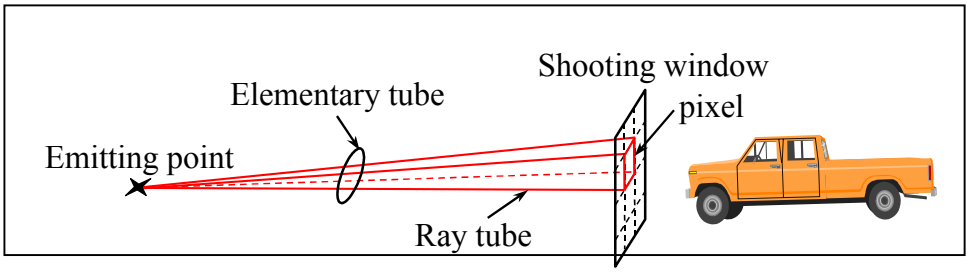

Figure 2: Shooting and bouncing rays technique

RADAR INTERACTION

Plane wave and clutter interaction

Each category of clutter is characterised by its backscattering coefficient average σ_0, which depends on the incidence angle and polarisation components (HH, VV, VH, and HV). But, real simulation values for σ are obtained by including statistical fluctuations (for speckle effects) using an exponential probability density function coupled with an uniform probability density function for the phase of backscattered field. This fluctuation is stored in each polygon as a texture pattern. Data on backscattering coefficients are extracted from (sparse) measurement campaigns published in literatures and F.T. Ulaby and M.C. Dobson‘s works [6]. An important synthesis task was performed in order to take into account frequency bands diversity and polarisation information. Contributions from all rays are summed up at a far-field observation point to obtain the final backscattered field from a definite area**.**

Plane wave and target interaction

High frequency asymptotic techniques and shooting rays technique were coupled in order to predict the backscattering field from complex targets [5]. To evaluate the multiple interactions, each ray is followed from one part of the target to another one. For large targets (according to the wavelength), the main contributions come from specular points at surfaces or edges. Thus, the RCS of complex targets can be predicted using the high frequency asymptotic approximations. Now, for facetted targets, two principal methods are applied: Physical Optics (PO) for surface scattering [4, 5, 7] and Geometrical Optics (GO) coupled with previous method to take into account multiple interactions. The shooting and bouncing rays technique performs very well in processing these interactions which can not be neglected because of their high return in wide aspect angle. Again, contributions from all rays are summed up at a far-field observation point to calculate the final backscattered field, eventually leading to the RCS of the target. This method is tested using examples of complex

vehicles such as jeep or tank and then, illustrate the necessity to take into account the multi-bounce effects in backscattering prediction.

Prospective work is ongoing in order to include edge diffraction [5, 8] using Physical Theory of Diffraction (PTD) or/and Uniform Theory of diffraction (UTD) and the coupling between such methods and GO. Thus, the scattering of intercepted surfaces throughout the multiple bounces, edge diffraction, reflection(s)-diffraction and/or diffraction-reflection(s) coupling could be considered.

Radar propagation

Attenuation due to vegetation and meteorological parameters has been taken into account. Both effects are predicted by applying the recommendations in 1986 and 1992 of the CCIR (Comité Consultatif International des Radiotélécommunications) in Geneva respectively. The vegetation model was improved after a comparison with a database of measurements for the cases of vegetation with and without leaves [10]. The atmospheric effects cover oxygen and water vapour absorption; clouds, haze, fog, and different intensities of rain attenuation.

Radar parameters

The principles used in the radar sensor modelling are flexible and thus preserve the evolutionary concept. This modelling transforms the field in front of the antenna into parameters such as range, radial velocity and angles. Then, this domain is processed according to specific procedures and operating modes. The performed simulation is developed from the matched filter theory and the associated ambiguity function. This approach based on energetic concepts (maximising signal-to-noise ratio for a known signal) is applied on all standard radar systems.

Antenna

Various antenna models are under consideration according to specific objectives, practical applications and aspect angle coverage requirements.

EXPLOITATION – UTILISATION

Radar cross section calculations

As shown on figure 3 on a generic target (here a virtual 3D helicopter) at 35 GHz, Radar Cross Section (RCS) calculations are achieved using the principles previously presented. Multi-bounce contributions are taken into account in this case. The main objective is a restitution of the realistic mean RCS coupled with its fluctuations.

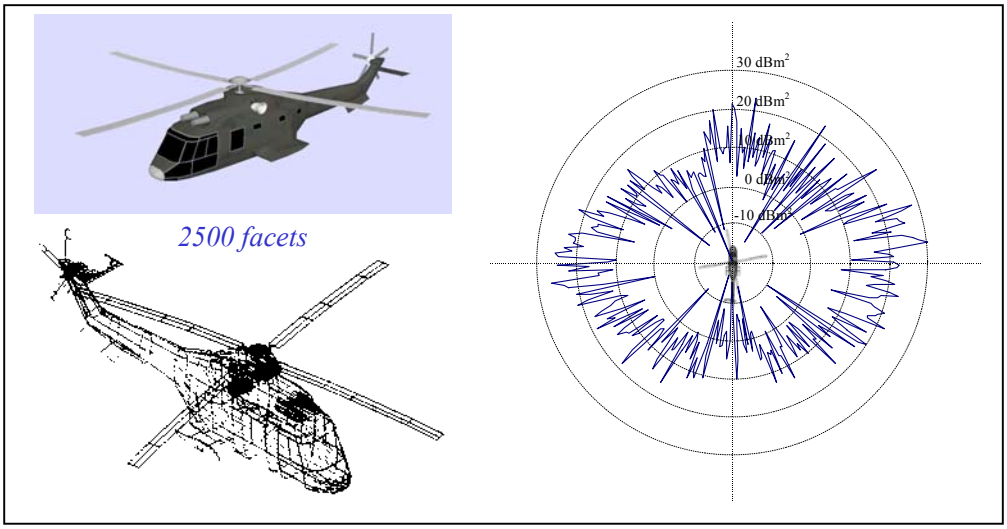

Figure 3: RCS of virtual 3D helicopter at 35 GHz

An example of millimetre wave modelling facilities on a 25000 facetted armoured repair and recovery vehicle has been performed. Time calculation is around 6 minutes for each range profile (obtained from 200 synthesised frequencies) on a standard workstation. Measurements were performed concerning this target. Very satisfying agreements between calculations and experimental results were observed in terms of RCS and Inverse Synthetic Aperture Radar (ISAR) imagery.

SAR simulation

In this particular case of SAR simulation, the illustrated calculations on figure 4 have been conducted using the following parameters:

- flight altitude of the carrier: 2 000 m
- image area: around 2 km x 2 km
- synthetic antenna beamwidth: 0.032°
- elevation beamwidth: 13°
- incidence angle: 63°

1024 range gates of 2 m (i.e. range resolution) were used to calculate the image on figure 5

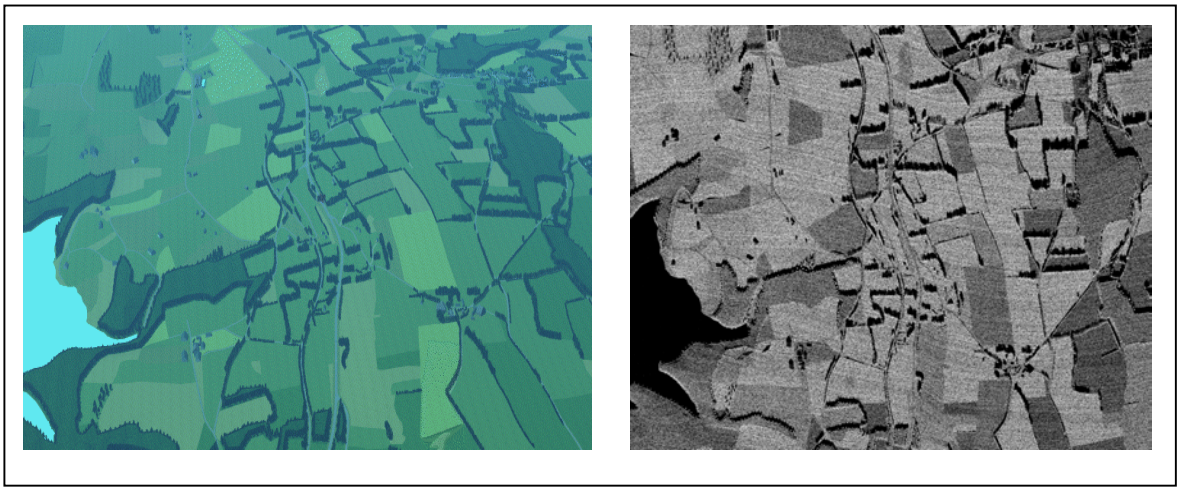

Figure 4: Specific area from database in optical domain and its SAR image simulation

Enhanced vision in airport context

The global project includes, among other subjects, enhanced vision using millimetre wave radar and infrared sensors imagery principally in poor weather conditions (haze, fog, rain). In order to evaluate the contribution of high resolution multisensor system in the airport context, simulations have been conducted on virtual airport database (ie Toulouse Blagnac airport **area).**

Results at 500 m from the touch down zone in front of the runway is shown on figure 5 for a simulated 94 GHz radar. Images have been calculated on a field of 30º (azimuth) by 10º (elevation). The antenna beamwidth is 0.15º in azimuth and 10º in elevation. The range gates are summed up in each 0.15º in elevation to obtain square pixels on such figure. This is chosen in order to achieve the same resolution both in cross range and along range. For each resolution cell or pixel, coherent summation of the different contributions from clutter and targets were performed according to the principles described above. To limit speckle fluctuations , average of 10 uncorrelated images are calculated and displayed.

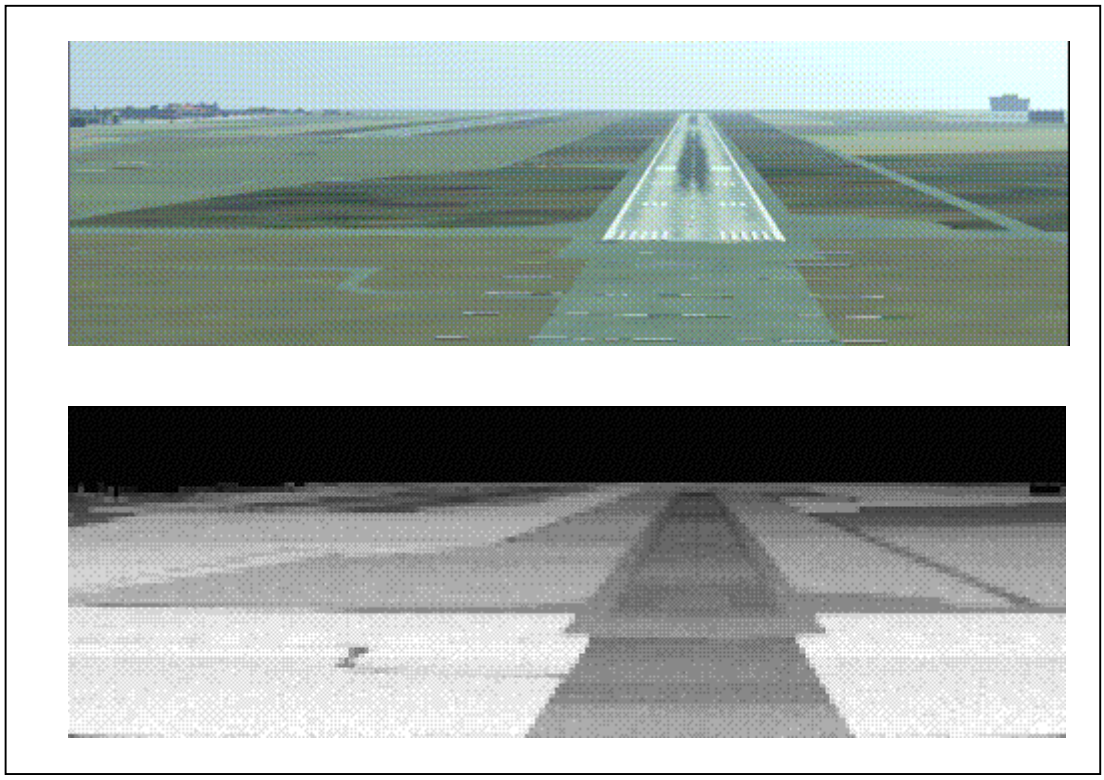

Figure 5: Visible and 94 GHz radar image simulation – 500 m from touch down zone

Airborne Radar in multisensor scenarios

The different processing steps are described in 4.2 section. This last application emphasised the wide possibility in the display of the results. Generally, imagery sequences generated by the radar transfer function are displayed using 2-D or 3-D visualisation tools. The visualised output data are voxels, which contain information about backscattering strength, angles information, distance and velocity. As shown on figure 6, the information is synthesised on a map.

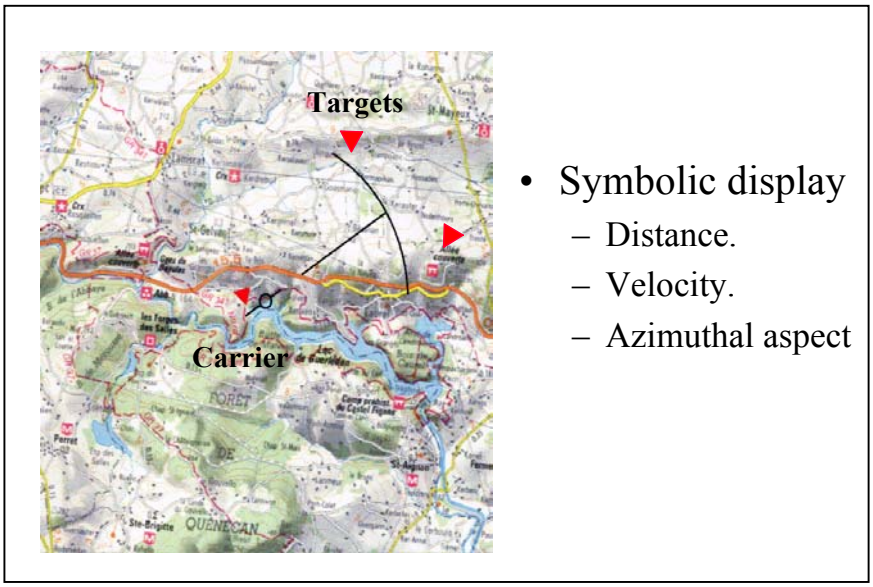

Figure 6: Example of visualisation display

SUMMARY AND PROSPECTS

Plane wave and target (or clutter in realistic database) interaction using SBR technique and high frequency asymptotic formulations have been presented in this paper. Taking the opportunity of various studies in this domain, a radar simulation package is under development. The simulation tool provides realistic calculations (RCS, 2-D SAR image, …) for complex geometry or database coupled with realistic scenarios. Future prospects intend to take into account target description by parametric surfaces, dielectric layers on or material loading in the targets and roughness of the target surfaces. Moreover research is ongoing on strong coupling between target and its immediate environment for other potential applications on radar imagery.

References

[1] P. Pitot, "The Voxar Project",
IEEE Comp. Graph. Appl., January 1993, pp.27-33.

[2] J. Latger, J.F. Talaron, "A useful kernel to make realistic infrared simulation",
ITEC'98.

[3] J. Latger, J.F. Talaron, "ONDE, a numerical tool for describing environment",
Defence and Optronics symposium'96.

[4] H. Ling, R.C. Chou, S.W. Lee "Shooting and Bouncing Rays: Calculating the RCS of an Arbitrarily Shaped Cavity"
IEEE Trans. Ant. Prop., Vol. 37, N°2, Feb. 1989, pp. 194-205.

[5] G. Ramière, P. Pitot, P.F. Combes, H.J. Mametsa "Shooting Ray and Multiple Interaction Coupling for Complex 3-D Radar Cross Section Predictions"
Radar 99 Conference, Brest (France), May 99.

[6] F.T. Ulaby, M.C. Dobson "Handbook of Radar Scattering Statistics for Terrain"
Artech House 1989

[7] G.T. Ruck, D.E. Barrick, W.D. Stuart, C.K. Krichbaum "Radar Cross Section Handbook"
Plenum Press, New York – London 1970

[8] A. Michaeli, "Elimination of infinities in equivalent edge currents, Part I: Fringe currents components", IEEE Trans. Antennas and Propagation, Vol. AP-34, 1986, pp. 912-918.

[10] A. Seville "Vegetation Attenuation: Modelling and Measurements at Millimetric Frequencies"
10th International Conference on Antenna and Propagation, 14-17 April 1997.

2) IGARSS'02 TORONTO (INTERNATIONAL GEOSCIENCE AND REMOTE SENSING SYMPOSIUM)

Application of IEM and Radiative Transfer Formulations for Bistatic Scattering of Rough Surfaces

H. J. Mametsa[1], F. Koudogbo[1,2], P. F. Combes[2]

[1]ONERA-DEMR
2, av. E. Belin, BP 4025
31055 Toulouse Cedex (France)
☎ : 33 5 62 25 27 07
✉ : mametsa@onecert.fr, koudogbo@onecert.fr

[2]UPS-AD2M-LGET
118, route de Narbonne
31062 Toulouse Cedex (France)
☎ : 33 5 62 25 27 13
✉ : pcombes@cict.fr

Abstract* - Systematic characterization of scattering behavior of natural and manmade rough surfaces is required in many radar applications. In general, the overall scattering response of such surfaces is composed of surface and volume scattering components. In this paper Integral Equation Method (IEM) is outlined to work out the *surface scattering* and the radiative transfer theory is applied to model the *volume scattering.

I. INTRODUCTION

Rigorous modeling of electromagnetic waves scattering from natural or artificial rough surfaces (ocean, sand, soils, snow, concrete, asphalt roads, …) is of great interest in many fields of applications. The scattering elements of such surfaces have complex geometry and are randomly distributed. So, their radar scattering involves complex interactions. At the millimeter waves, semi-empirical models and sparse measurements encountered in the literature are not in good agreement and it is not practical to evaluate the scattered fields by exact or asymptotic electromagnetic methods.
In this paper, we propose and set out rigorous analytical formulations to calculate the scattered power by rough surfaces: the IEM method for surface scattering and the radiative transfer theory for volume scattering. These models take into account the statistical description of the surface and are valid over a wide range of surface roughness.

II. ROUGH SURFACE DESCRIPTION

The surface roughness is usually described by a statistical distribution. Two principal parameters characterize the surface [1]: the root mean square of surface heights s_z and the correlation length l_c which describes the density of the irregularities. Most methods usually assume that the surface height distribution p(z) is gaussian. Nevertheless, s_z alone is not enough to completely describe a surface roughness. Several profiles could have the same height distribution but could present noticeable difference in the spatial variation of the irregularities. This difference is characterized by the correlation function ρ(r). Gaussian and exponential functions are often proposed in theoretical modeling. The correlation length l_c is the given distance where the correlation function is equal to $1/e = 0.368$. In fact and more precisely, the scattering behavior respectively depends on the values of ks_z and kl_c, k is the wave number given by $2\pi/\lambda$.

III. INTEGRAL EQUATION METHOD

A. Classical asymptotic methods [1], [2], [3]

The small perturbation model (SPM) could be used for small values of such aforementioned parameters: $ks_z < 0.3$ and $kl_c \leq 3$. It assumes that the scattered electromagnetic field could be represented by a superposition of plane waves of unknown amplitudes which are propagated towards the receiver.

The Kirchhoff model (KM) considers that each point of the analyzed rough surface belongs to the infinite tangent plane to the surface at this point. This method must be used within the following restrictions: $ks_z \leq 1.5$ and $kl_c > 2\pi$.

Although these methods are the most common techniques for computing the scattered electromagnetic field from rough surfaces, their efficiency is restricted to small roughness or long correlation length surfaces. Fig. 1 summarizes their range of validity. Previous limitations are circumvented by using the Integral Equation Model (IEM) for the surface scattering coefficient. Its range of validity overlaps those of KM and SPM (Fig. 1).

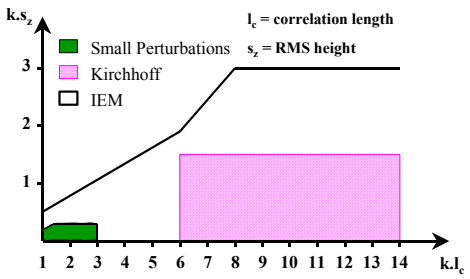

Fig 1: Range of validity

B. IEM formulation [4], [5]

The IEM model gives a solution of the Stratton-Chu integral equation: the scattered field is obtained by a reformulation of the tangential field through two components: the Kirchhoff term and a complementary term (1). Recent formulations from J.L. ALVAREZ-PEREZ [5] have been taken into account. From this consistent IEM formulation, rigorous description of the multiple scattering mechanisms has been developed in order to evaluate the coherent and incoherent scattering coefficients (Fig. 2) and the crosspolarization terms even in the complex monostatic configuration.

$$E^s_{qp} = E^{sk}_{qp} + E^{sc}_{qp} \tag{1}$$

p et q respectively denote the polarization of the transmitting and receiving antennas.

The coherent scattered power (power scattered in the specular lobe) is calculated from the mean squared power (2) and the incoherent contribution is obtained by subtracting the previous coherent power from the total power (3).

$$P^s_{qp_{coh}} = \frac{1}{2\eta}\left\langle E^{sc}_{qp}\right\rangle\left\langle E^{sc*}_{qp}\right\rangle = \frac{1}{2\eta}\left\langle E^{sk}_{qp}\right\rangle\left\langle E^{sk*}_{qp}\right\rangle + \frac{1}{2\eta}2\Re e\left[\left\langle E^{sc}_{qp}\right\rangle\left\langle E^{sk*}_{qp}\right\rangle\right] + \frac{1}{2\eta}\left\langle E^{sc}_{qp}\right\rangle\left\langle E^{sc*}_{qp}\right\rangle \tag{2}$$

$$P^s_{qp_{incoh}} = \frac{1}{2\eta}\left[\left\langle E^s_{qp}E^{s*}_{qp}\right\rangle - \left\langle E^s_{qp}\right\rangle\left\langle E^{s*}_{qp}\right\rangle\right] \tag{3}$$

η is the impedance in the medium.

Note that the dimensionless scattering coefficient, depending on the scattered and incident power, is given by (4).

$$\sigma^s_{qp} = \frac{4\pi R^2 P^s_{qp}}{A_0 P^i_{qp}} \tag{4}$$

where P^i_{qp} and P^s_{qp} are respectively the incident and scattered power; and A_0 is the illuminated surface. Fig. 2 presents the different components of the total scattered power.

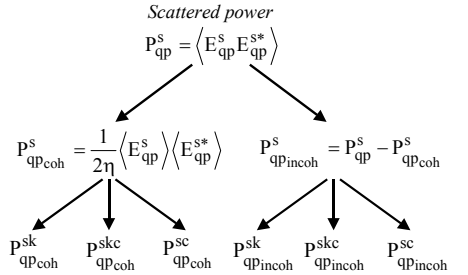

Fig. 2 : Total scattered power by IEM model

C. IEM results

1) Backscattering

Our first application results concern the backscattering coefficient formulation at millimeter wave frequencies (35 and 94 GHz) for asphalt and concrete roads. Good agreement between theoretical results and measurements found out in literature is established (Fig. 3) [4]. Interesting results are also obtained for the particular and original case of grazing incidence between 70º and 88º (Fig. 3). Sparse results are present in relative bibliography concerning this incidence. So, validation is still under investigation [2], [4], [6].

2) Bistatic scattering

In bistatic scattering problem, Fig. 4 shows the variations relative to roughness of the coherent and incoherent components of the scattered power from an asphalt road at 94 GHz. The incident angle is -40˚. On smooth surface, total incident power is scattered in the main lobe of reflection. Higher roughness leads to lower coherent diffracted power and an increasing of the incoherent component.

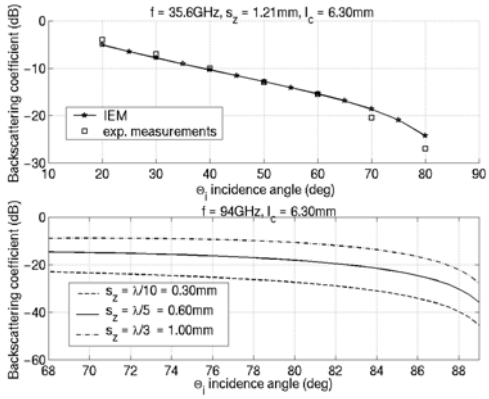

Fig. 3 : Backscattering coefficient from asphalt

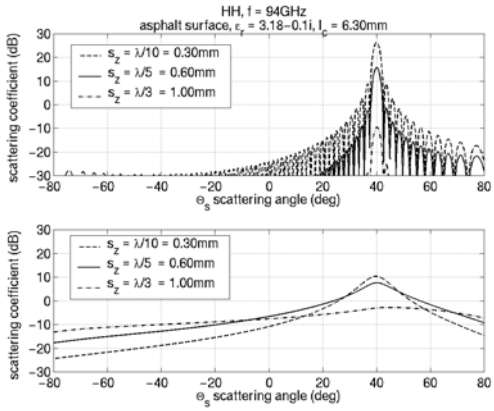

Fig. 4 : Coherent and incoherent bistatic scattering from asphalt at 94GHz

IV. RADIATIVE TRANFERT THEORY

A. Formulation [4], [6]

The radiative transfer theory deals with the transport of energy through a medium containing particles. It accounts the Stokes vector variations of an electromagnetic wave propagating through a random medium composed of clusters embedded in a host medium. These variations are due to different phenomena: absorption losses by the host medium and the particles, scattering losses by the particles and thermal emission by the global inhomogeneous medium. The scattering coefficient is obtained by solving the radiative

transfer differential equation (4) which governs the wave propagation in the medium.

$$\frac{d\vec{I}(\vec{r},\hat{s})}{ds} = -\kappa_e I(\vec{r},\hat{s}) + \vec{J}_e(\vec{r}) + \int_{4\pi} d\Omega' P(\hat{s},\hat{s}') I(\vec{r},\hat{s}') \qquad (4)$$

This equation is formulated in terms of three constitutive functions:

- κ_e, the extinction matrix, describes the attenuation of the intensity due to absorption and scattering.
- $\vec{J}_e$ is a source function that accounts for self thermal emission in the medium. In radar remote sensing, its contribution is small in comparison with the other terms and it is neglected.
- P is the 4x4 phase matrix. It specifies the angular distribution of the incident intensity from a given direction into other directions.

The intensity I_q^s scattered in a given direction is found out by solving the radiative transfer differential equation above. With the incident intensity I_p^i, equation (5) below gives the volume scattering coefficient [6].

$$\sigma_{qp}^0 = \frac{4\pi \cos\theta_s * I_q{}^s(\theta_s,\varphi_s)}{I_p{}^i(\theta_i,\varphi_i)}, \qquad (5)$$

B. Radiative transfer equation results

The backscattering (HH, VV, HV, VH) and bistatic scattering coefficients obtained from (4) and (5) are shown on Fig. 5.

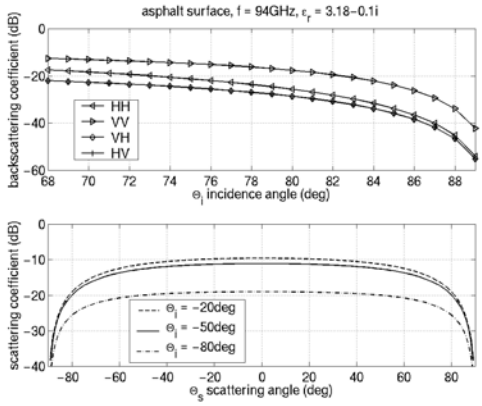

Fig 5 : Asphalt volume scattering coefficients

V. TOTAL BACKSCATTERING COEFFICIENT

A. Grazing incidence in backscattering

In response to large requirements in modeling from remote sensing up to safety in road transportation, bistatic scattering coefficients are calculated from the nadir to the hardly developed grazing incidence, at millimeter waves. Thus, the first application is focused on road surfaces such as asphalt and concrete. Surface and volume contributions are summed up to obtain the total backscattering coefficient [6]. For the volume contribution calculations, the incident power is only the part of power transmitted in the host medium. Results are shown on Fig. 6. Validation is achieved using experimental results in literature [6].

B Bistatic scattering case

Surface and volume contributions are summed up to obtain the total bistatic scattering coefficient. Fig. 6 shows that the volume contribution is preponderant in directions far away from the specular direction. The incident angle is -40°. At $s_z = \lambda/3$, volume scattering is lower than the surface scattering. For higher values of s_z, the volume scattering could be neglected in comparison with the surface scattering.

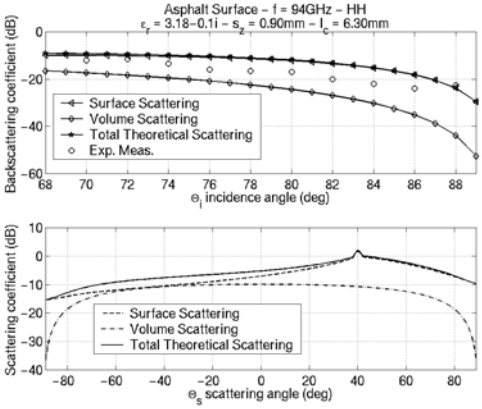

Fig 6 : HH asphalt total scattering coefficients

VII. CONCLUSION

In this paper, a general bistatic scattering electromagnetic model derived from the IEM (surface scattering) and the radiative transfer formulation (volume scattering) has been evaluated. Interesting results were obtained even for the particular case of grazing incidence between 70º and 88º. Theoretical results and measurements found out in appropriate papers are in good agreement. Theoretical modeling of radar sensor usually deals with the modeling of the Radar Cross Section (RCS) of targets and the modeling of the terrain scattering coefficient. Our current studies investigate the coupling of the targets and their immediate environment using both the bistatic scattering coefficients from the target and the terrain around it.

REFERENCES

[1] J. A. OGILVY, « Theory of wave scattering from random rough surfaces », *Adam Hilger*,1991.

[2] F.T ULABY, R.K MOORE, A.K FUNK, « Microwave remote sensing active and passive – vol II et III », *Artech House*, 1982 et 1986.

[3] P. BECKMANN, A. SPIZZICHINO, « The scattering of electromagnetic waves from rough surfaces », *Pergamon Press*, 1963.

[4] A.K. FUNG, « Microwave scattering and emission models and their applications », Artech House, 1994.

[5] J.L. ALVAREZ-PEREZ, « An extension of the IEM/IEMM surface scattering model », *Waves Random Media*, vol. 11, pp. 307-329, 2001
[6] E.S. LI, K. SARABANDI, « Low grazing incidence millimeter-wave scattering models and measurements for various from road surfaces », *IEEE Trans. AP*, vol. 47, pp. 851-861, 1999.
[7] G. MARCELLONI & al., « Experimental validation of the surface scattering and emission models. », *IEEE Trans. GRS*, vol. 38, n°1, pp. 459-469, 2000